MgB_2 thin films fabricated on Fe tape and effects of annealing on their properties

Akira Yamasaki[1], Hiroto Kambe[1], Iwao Kawayama[1], Ataru Ichinose[2], and Toshiya Doi[1,*]

[1]*Graduate School of Energy Science, Kyoto University, Kyoto 606-8501, Japan*

[2]*Central Research Institute of Electric Power Industry, Yokosuka, Kanagawa 240-0196, Japan*

E-mail: doi.toshiya.8c@kyoto-u.ac.jp

Magnesium diboride (MgB_2) thin films were fabricated on Fe tapes by an electron-beam evaporation method and post-annealed at 650 °C for 1–5 h. Appropriate post annealing (1 h) resulted in a critical temperature (T_c) of 34.4 K and infield critical current density (J_c) of 0.20 MA/cm^2 at 20 K under 6 T. Characterization suggests that annealing improves the crystallinity of the MgB_2 thin film; however, Fe diffuses into the MgB_2 layer when annealing for longer durations, which deteriorates the superconductivity. MgB_2 thin films on Fe tape can be utilized in diverse superconducting applications under external magnetic fields.

Magnesium diboride (MgB_2), in recent years, has gained increasing attention. It offers several benefits for practical applications over conventional superconductors, such as Nb–Ti and Nb_3Sn, and high-temperature superconductors (HTSs), such as $YBa_2Cu_3O_7$ and $(Bi,Pb)_2Sr_2Ca_2Cu_3O_{10}$. MgB_2 has a superconducting critical temperature (T_c) of 39 K,[1] which is higher than those of conventional metallic superconductors; this enables the liquid-helium free operation of MgB_2 at 20 K using a suitable cryocooler or liquid-hydrogen cooling. MgB_2 can offer low-cost and lightweight superconducting tapes considering the abundance and low specific gravities of the constituent elements Mg and B. Additionally, crystal orientation is not required to produce MgB_2 wires,[2] contrary to $(Bi,Pb)_2Sr_2Ca_2Cu_3O_{10}$ and $YBa_2Cu_3O_7$ in which uniaxial and biaxial orientations are required, respectively. Furthermore, the grain boundaries of MgB_2 work as vortex pinning centers that improve the infield critical current density (J_c),[3] whereas artificial pinning centers must be introduced into HTSs.

Extensive studies have been conducted on fabricating high performance MgB_2 superconducting wires using powder-in-tube (PIT) techniques involving in-situ,[4] ex-situ,[5] and internal Mg diffusion processes.[6] However, these methods result in a low filling factor as well as formation of magnesium oxides at the grain boundaries.[7] Consequently, the J_c's of PIT-processed MgB_2 wires at 20 K are significantly lower than those of Nb–Ti wires at 4.2 K.

Several vacuum deposition techniques have been explored for the preparation of MgB_2 thin film, including pulsed laser deposition,[8] molecular-beam epitaxy,[9] electron-beam evaporation (EBE),[10] hybrid physical–chemical vapor deposition (HPCVD),[11] radio frequency (RF) magnetron sputtering,[12] and reactive evaporation.[13] The deposition of MgB_2 under vacuum results in a near-perfect relative density and suppresses the oxidation of Mg, leading to an increased J_c. The J_c's of MgB_2 thin films are generally more than 10 times higher than those of PIT-processed wires. High-quality MgB_2 films exhibiting a self-field J_c of approximately 100 MA/cm^2 at 20 K have been fabricated by HPCVD;[14] however, their J_c's decreased to approximately 0.5 MA/cm^2 under a magnetic field of 1.5 T, which is similar to that of PIT-processed MgB_2 wires. Furthermore, their upper critical fields (B_{c2}) at 20 K were less than 2 T. In another study, MgB_2 thin films fabricated by EBE exhibited an infield J_c of 0.2 MA/cm^2 at 20 K under a magnetic field of 3 T.[15] These results were attributed to the columnar MgB_2 grains with a diameter of approximately 10 nm with low crystallinity induced by low-temperature growth. Although the grain boundaries among adjacent grains work as strong vortex-pinning centers,[3] enhancement of the J_c at 20 K still remains a

challenge.

High-temperature post-annealing has been found to improve the infield J_c of MgB_2 films in magnetic fields.[16,17] In our previous study,[17] an MgB_2 thin film was prepared on a single-crystal Si substrate using EBE at a substrate temperature of 280 °C, followed by the deposition of a Nb protective layer by RF sputtering method. The film, annealed at 650 °C for 1 h, exhibited a T_c of 37.5 K and a J_c of 1.4 MA/cm^2 at 20 K under 6 T.[17] Although the T_c of the thin film was comparable to that of PIT-processed MgB_2 wires, the infield J_c was more than 100 times and several ten-fold higher than that of PIT-processed MgB_2 wires and the as-grown MgB_2 film, respectively.[17] Thus, annealing at 650 °C with a Nb protective layer can increase both the T_c and infield J_c of MgB_2 thin films.

For practical applications, it is important to prepare MgB_2 thin films on metal substrates, which in turn enables the fabrication of MgB_2 superconducting wires using thin film techniques. Thus, in this study, we aimed at preparing MgB_2 superconducting thin films on metal tape. Candidate metal substrates include common metals like Fe, Cu, and Al. Among these, Al is unsuitable because the post-annealing temperature of 650 °C is close to the melting point of Al. Cu is also not suitable because preliminary experiments with a Cu/MgB_2/B/Si sample demonstrated that post-annealing at 650 °C for 1 h decreased the T_c and J_c significantly owing to a reaction between MgB_2 and Cu. Therefore, Fe was chosen here as the metal substrate.

An MgB_2 thin film was prepared on a Fe substrate (20 mm × 20 mm × 0.5 mm) by EBE. The base pressure of the EBE chamber was less than 1.0×10^{-7} Pa. The substrate was heated at 280 °C using a halogen heater during the deposition in the EBE chamber. A block of Mg (99.9%) and granular B (99.5%) were used as raw materials. The flux rates of Mg and B were manually controlled using quartz crystal monitors, and the deposition rate of MgB_2 was maintained at 0.6 nm/s. When the shutter of the B source was opened, the substrate temperature rapidly increased by ~10 °C owing to thermal radiation from the B source. If the substrate temperature changes during MgB_2 deposition, it affects the amount of Mg that re-evaporates; consequently, the as-grown MgB_2 thin film would have a non-uniform composition. Therefore, the B shutter was opened first, and a B layer was deposited for 270 s until the substrate temperature reached a stable level. Then, the Mg shutter was opened to facilitate the deposition of the MgB_2 film for 300 s. After the deposition of the MgB_2 thin film, a 10-nm-thick Nb layer was deposited in the EBE chamber using an arc plasma gun to prevent oxidation of MgB_2 during sample transfer to a sputtering chamber. The sample was then taken out from the EBE chamber into the atmosphere and placed in a sputtering chamber,

in which a 6-μm-thick Nb layer was deposited to prevent oxidation of the MgB_2 thin film and Mg re-evaporation during post-annealing.

The prepared Nb/MgB_2/B/Fe sample (20 mm × 20 mm × 0.5 mm) was cut into small pieces of 10 mm × 4 mm × 0.5 mm. The pieces were placed in alumina crucibles with lids, wrapped in Al foil, and placed in Fe crucibles with lids. The Fe crucibles were heated in a vacuum furnace at 650 °C and approximately 60 Pa vacuum for 1, 3, or 5 h for post-annealing.

The crystalline phases in the thin films were determined using θ–2θ X-ray diffraction (XRD) measurement. J_c and T_c were measured using a four-probe method using a Physical Property Measurement System (PPMS; Quantum Design, Inc., California, USA). For J_c measurements, the temperature and external magnetic field were 20 K and 0–6 T, respectively. The magnetic field was applied perpendicular to the film surface. The cross-sectional microstructures and elemental distribution of the thin films were observed by bright-field scanning transmission electron microscopy (BF-STEM) and energy-dispersive X-ray spectroscopy (EDS), respectively.

Figure 1 shows the XRD patterns of the non-annealed sample, annealed samples (650 °C for 1, 3, and 5 h), and Fe substrate. The Nb(110) peak, which was observed for all the Nb/MgB_2/B/Fe samples, indicates the existence of the Nb protective layer. As the annealing time increased, this peak shifted toward a lower angle. In addition, after annealing for 3–5 h, a NbO(111) peak appeared, which became stronger as the annealing time increased. This suggests that the Nb protective layer was slightly oxidized during the annealing process. MgB_2(002) peaks were not observed for any of the samples, in contrast to our previous study,[17] in which MgB_2(002) peaks were observed in the XRD patterns of Nb/MgB_2/B/Si samples. This could be because the Nb protective layer in this study was thicker than that in the previous study[17] (6 vs. 3 μm). Nb (110) peaks can be observed in all the samples whereas the small peaks of NbO (111) were seen only in the samples annealed for 3 h and 5 h. Presence of sufficient metal Nb and significantly small generation of NbO and Nb_2O_5 phases after the annealing indicates that Nb layers blocked the oxygen diffusion from the atmosphere to the MgB_2 layer during the post annealing.

Figure 2 shows the temperature dependence of the resistivity of the non-annealed and annealed MgB_2 thin films and Fe substrate. There was an unexpected peak at around 34 K for the non-annealed sample, which was attributed to the presence of Inconel in the measuring equipment (PPMS).[18] The zero-resistivity ($\rho < 0.5$ μΩ·cm) T_c of the non-annealed and annealed samples (1, 3, and 5 h) were 33.5, 34.4, 28.8, and 24.1 K, respectively. Notably, annealing for 1 h increased the T_c compared to that of the non-annealed sample.

This is because annealing increases the crystallinity of the MgB_2 layer.[17] Conversely, the T_c values of the samples annealed for 3 and 5 h were lower than that of the non-annealed sample. The resistivities of the MgB_2 samples annealed for 3 and 5 h were similar to that of the Fe substrate and lower than those of the non-annealed and 1-h-annealed samples. This suggests that the resistivity of the B layer decreases due to the diffusion of Mg atoms into the B layer by annealing for 3–5 h; thus, the measurement current flows from the current terminal on the Nb layer to the Fe substrate through the MgB_2 and B layers.

Figure 3 demonstrates the magnetic-field dependence of the J_c's of the MgB_2 thin films at 20 K. The reported results of PIT-processed MgB_2 wires,[19] MgB_2 films prepared using HPCVD,[14] and non-annealed and annealed (650 °C for 1 h) MgB_2 films prepared on Si using EBE[17] are also shown for comparison. The magnetic field (0–6 T) was applied perpendicular to the film surface. The J_c's of the non-annealed Nb/MgB_2/B/Fe sample could not be measured at 0 and 0.1 T because the critical current (I_c) exceeded the set value of the current source. The I_c of the 3-h-annealed Nb/MgB_2/B/Fe sample at 5–6 T was too low to determine accurately. The J_c of the non-annealed sample under all magnetic fields (0.5–6 T) was similar to that of the non-annealed MgB_2 thin film prepared on Si. This indicates that the quality of the as-grown Nb/MgB_2/B/Fe and Nb/MgB_2/B/Si[17] samples is comparable. The J_c of the 1-h-annealed Nb/MgB_2/B/Fe sample were slightly lower than those of the non-annealed sample under magnetic fields of 0.5–3.0 T; however, under magnetic fields above 3.5 T, the J_c values were higher. This is attributed to the improved crystallinity of the MgB_2 layer after annealing. This is different to the case of the Nb/MgB_2/B/Si samples,[17] wherein annealing for 1 h improved the J_c values under all magnetic fields (0–6 T). The J_c values of the 3-h-annealed Nb/MgB_2/B/Fe sample were lower than those of the 1-h-annealed sample annealed for 1 h in under all magnetic fields. The J_c values of the 5-h-annealed Nb/MgB_2/B/Fe sample were zero under all magnetic fields. These results indicate that diffusion of some impurity element into the MgB_2 layer occurred during annealing.

To investigate the effect of annealing on the diffusion, the cross-sections of the non-annealed and 5-h-annealed Nb/MgB_2/B/Fe samples were analyzed by STEM-EDS. The BF-STEM images and EDS elemental maps (Nb, Mg, B, O, and Fe) of the non-annealed and 5-h-annealed samples are shown in Figures 4(a) and 4(b), respectively, while the EDS line profiles (Nb, Mg, B, O, and Fe) are shown in Figures 5(a) and 5(b), respectively. Each layer was clearly visible in the BF-STEM images; the thicknesses of the B, MgB_2, and Nb layers were 90, 175, and 6000 nm, respectively. At the B/Fe interface, there was a thin O-rich layer with approximately 10 at.% O, indicating the presence of a very thin native oxide layer on

the surface of the Fe substrate. In addition, after annealing for 5 h, there was an O-rich layer with approximately 10 at.% O at the Nb/MgB_2 interface, indicating the generation of an oxide layer during annealing. A similar phenomenon occurred in the Nb/MgB_2/B/Si samples after annealing at 650 °C for 1 h.[17] The EDS results indicated that the B content was approximately 50 at.% in the Nb layer; however, this is only an artifact of the measurement, because the characteristic X-rays emitted from B and Nb overlap (0.1833 keV for the B Kα line and 0.1717 and 0.1718 keV for the Nb M line). No diffusion of B into the Nb layer was actually considered to take place. Before annealing, the composition ratio of Mg and B was uneven (Figure 5(a)), indicating that the flux rates of Mg and B, or the temperature of the substrate during fabrication, were not constant. Conversely, the composition ratio of Mg and B after annealing was uniform (Figure 5(b)), suggesting that the mutual diffusion of Mg and B atoms in the MgB_2 layer during annealing might improve T_c and J_c. Mg diffusion from the MgB_2 layer into the B layer was also reported previously.[17] Thus, these observation results do not explain why the T_c and J_c values of the Nb/MgB_2/B/Fe samples decreased after annealing for 3–5 h.

Although there was no evident diffusion of Fe or Nb into the MgB_2 layer during annealing, the Fe substrate or protective Nb layer could be responsible for the decreased T_c and J_c values after annealing for 3–5 h. To further investigate the decrease in T_c and J_c of the Nb/MgB_2/B/Fe samples annealed for 3–5 h, a Nb/MgB_2/B/Si thin film was synthesized (using a single-crystal Si substrate instead of Fe). The prepared Nb/MgB_2/B/Si sample was cut into pieces of 10 mm × 4 mm × 0.5 mm, and annealed at 650 °C for 0.5–10 h. The zero-resistivity T_c values of the non-annealed and annealed samples (0.5, 1, 2, and 10 h) were 35.5, 36.9, 36.9, 36.9, and 37.0 K, respectively. Thus, in contrast to the Nb/MgB_2/B/Fe sample, the T_c of the Nb/MgB_2/B/Si thin film increases monotonically after annealing. This suggests that the decrease in T_c and J_c of the Nb/MgB_2/B/Fe sample after annealing at 650 °C for 3–5 h is related to the use of the Fe substrate, not the protective Nb layer. Although Fe was not detected in the MgB_2 layer in the EDS analysis, it is speculated that a small amount of Fe from the Fe substrate diffuses through the B layer and into the MgB_2 layer during annealing, although the amount is below the sensitivity limit of the equipment used. Because Fe is a ferromagnetic element, even a small amount of Fe in the MgB_2 layer would decrease T_c and J_c.

In summary, while the crystallinity of the MgB_2 layer is improved by annealing at 650 °C, the superconductivity deteriorates owing to the diffusion of Fe through the B layer. Annealing for 1 h increases T_c and infield J_c at 3.5–6 T; however, annealing for 3–5 h

decreases them. After annealing at 650 °C for 1 h, the MgB_2 thin film on an Fe substrate had a T_c of 34.4 K and J_c of 0.20 MA/cm^2 at 20 K under a magnetic field of 6 T, which is seven times higher than that of a PIT-processed MgB_2 wire.[19] In comparison, an as-grown 10-μm-thick MgB_2 film on a Cu plate exhibited J_c values of 80, 7, and 0.09 MA/cm^2 at 20 K under 0, 3, and 6 T, respectively.[20] If a 10-μm-thick MgB_2 film were prepared on a 100-μm-thick Fe tape and annealed at 650 °C for 1 h, its engineering critical current density (J_e) would reach 0.018 MA/cm^2 at 20 K under 6 T. Unlike high-temperature superconductors, no particular crystal orientation is required to produce MgB_2 wires;[2] therefore, we can easily produce a thick MgB_2 layer with a very high deposition rate. This study may open a new research avenue for MgB_2-coated conductors using Fe tape for the practical application of superconductors in the field of magnetics.

References

1) J. Nagamatsu, N. Nakagawa, T. Muranaka, Y. Zenitani, and J. Akimitsu, Nature **410**, 63 (2001).

2) D. C. Larbalestier, L. D. Cooley, M. O. Rikel, A. A. Polyanskii, J. Jiang, S. Patnaik, X. Y. Cai, D. M. Feldmann, A. Gurevich, A. A. Squitieri, M. T. Naus, C. B. Eom, E. E. Hellstrom, R. J. Cava, K. A. Regan, N. Rogado, M. A. Hayward, T. He, J. S. Slusky, P. Khalifah, K. Inumaru, and M. Haas, Nature **410**, 186 (2001).

3) H. Kitaguchi, A. Matsumoto, H. Kumakura, T. Doi, H. Yamamoto, K. Saitoh, H. Sosiati, and S. Hata, Appl. Phys. Lett. **85**, 2842 (2004).

4) B. A. Glowacki, M. Majoros, M. Vickers, J. E. Evetts, Y. Shi, and I. McDougall, Supercond. Sci. Technol. **14**, 193 (2001).

5) S. Jin, H. Mavoori, C. Bower, and R. B. van Dover, Nature **411**, 563 (2001).

6) G. Giunchi, S. Ceresara, G. Ripamonti, A. Di Zenobio, S. Rossi, S. Chiarelli, M. Spadoni, R. Wesche, and P. L. Bruzzone, Supercond. Sci. Technol. **16**, 285 (2003).

7) J. H. Kim, S. X. Dou, D. Q. Shi, M. Rindfleisch, and M. Tomsic, Supercond. Sci. Technol. **20**, 1026 (2007).

8) W. N. Kang, H.-J. Kim, E.-M. Choi, C. U. Jung, and S.-I. Lee, Science **292**, 1521 (2001).

9) K. Ueda and M. Naito, Appl. Phys. Lett. **79**, 2046 (2001).

10) M. Okuzono, T. Doi, Y. Ishizaki, Y. Kobayashi, Y. Hakuraku, and H. Kitaguchi, IEEE Trans. Appl. Supercond. **15**, 3253 (2005).

11) X. Zeng, A. V. Pogrebnyakov, A. Kotcharov, J. E. Jones, X. X. Xi, E. M. Lysczek, J. M. Redwing, S. Xu, Q. Li, J. Lettieri, D. G. Schlom, W. Tian, X. Pan, and Z.-K. Liu, Nat. Mater. **1**, 35 (2002).

12) J.-R. Ahn, S.-G. Lee, Y. Hwang, G. Y. Sung, and D. K. Kim, Phys. C: Supercond. **388–389**, 127 (2003).

13) B. H. Moeckly and W. S. Ruby, Supercond. Sci. Technol. **19**, L21 (2006).

14) C. G. Zhuang, S. Meng, C. Y. Zhang, Q. R. Feng, Z. Z. Gan, H. Yang, Y. Jia, H. H. Wen, and X. X. Xi, J. Appl. Phys. **104**, 013924 (2008).

15) H. Kitaguchi, T. Doi, Y. Kobayashi, A. Matsumoto, H. Sosiati, S. Hata, M. Fukutomi, and H. Kumakura, IEEE Trans. Appl. Supercond. **15**, 3313 (2005).

16) S. Horii, A. Ichinose, T. Iwanaka, T. Kusunoki, and T. Doi, Appl. Phys. Express **11**, 093102 (2018).

17) H. Kambe, I. Kawayama, N. Kitamura, A. Ichinose, T. Iwanaka, T. Kusunoki, and T. Doi, Appl. Phys. Express **14**, 025504 (2021).

18) Quantum Design Inc., “Distorted low-level signal readback of AC signals in the PPMS in the temperature range 25-35 K due to Inconel mitigation of inductive cross talk,” https://www.qdusa.com/siteDocs/appNotes/AR04.pdf (Last accessed on September 7, 2022).
19) K. Togano, J. Hur, A. Matsumoto, and H. Kumakura, Supercond. Sci. Technol. **23**, 085002 (2010).
20) T. Kusunoki, H. Yamamoto, M. Kodama, H. Kotani, H. Tanaka, G. Nishijima, S. Horii, and T. Doi, IEEE Trans. Appl. Supercond. **27**, 6200204 (2017).

Figure captions

Fig. 1. XRD patterns of the non-annealed and annealed Nb/MgB_2/B/Fe samples and Fe substrate.

Fig. 2. Temperature dependence of the resistivities of the non-annealed and annealed Nb/MgB_2/B/Fe samples and Fe substrate.

Fig. 3. Magnetic-field dependence of the J_c’s of the non-annealed and annealed Nb/MgB_2/B/Fe samples.

Fig. 4. Cross-sectional BF-STEM images and EDS elemental mapping images (Nb, Mg, B, O, and Fe) of (a) non-annealed and (b) 5-h-annealed Nb/MgB_2/B/Fe samples.

Fig. 5. EDS line profiles of Nb, Mg, B, O, and Fe in (a) non-annealed and (b) 5-h-annealed Nb/MgB_2/B/Fe samples.

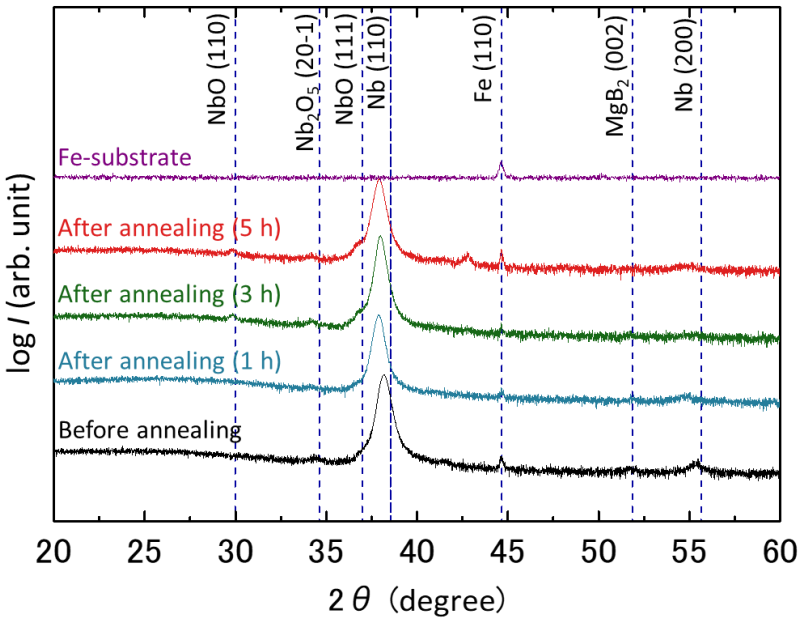
NbO (110)
Nb2O5 (20-1)
NbO (111)
Nb (110)
Fe (110)
MgB2 (002)
Nb (200)
Fe-substrate
After annealing (5 h)
After annealing (3 h)
After annealing (1 h)
Before annealing
log I (arb. unit)
20
25
30
35
40
45
50
55
60
2θ (degree)

Fig. 1

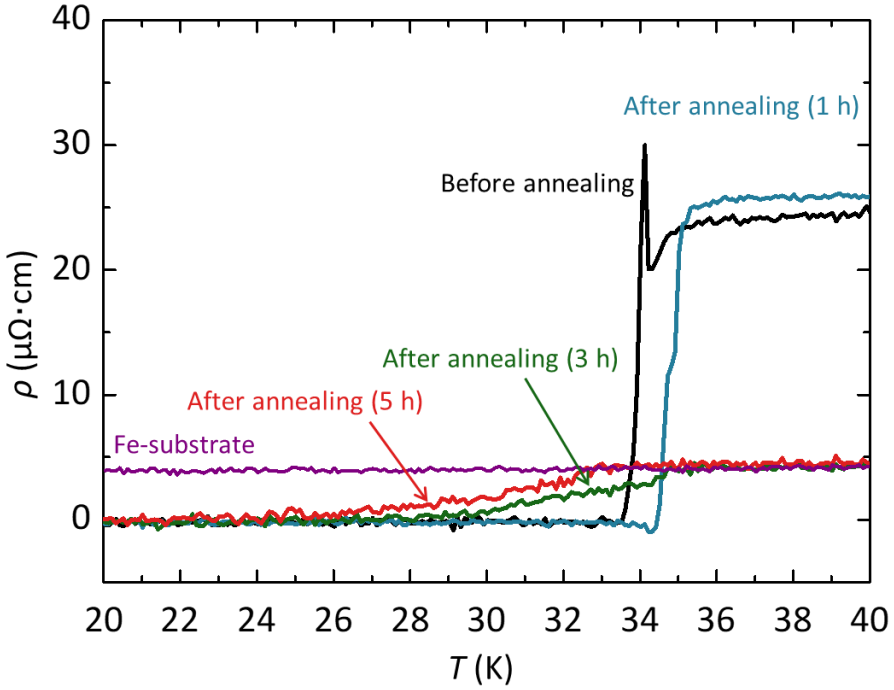
40
30
20
10
0
ρ (μΩ·cm)
20
22
24
26
28
30
32
34
36
38
40
T (K)
After annealing (1 h)
Before annealing
After annealing (3 h)
After annealing (5 h)
Fe-substrate

Fig. 2

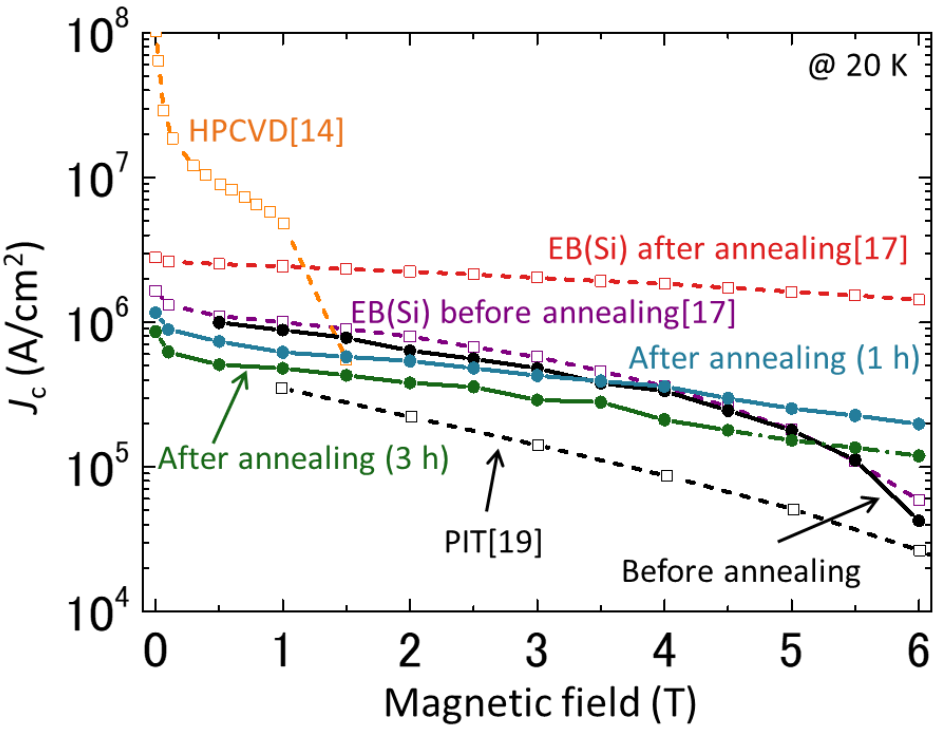
@ 20 K
HPCVD[14]
EB(Si) after annealing[17]
EB(Si) before annealing[17]
After annealing (1 h)
After annealing (3 h)
PIT[19]
Before annealing
J_c (A/cm^2)
Magnetic field (T)
10^8
10^7
10^6
10^5
10^4
0
1
2
3
4
5
6

Fig. 3

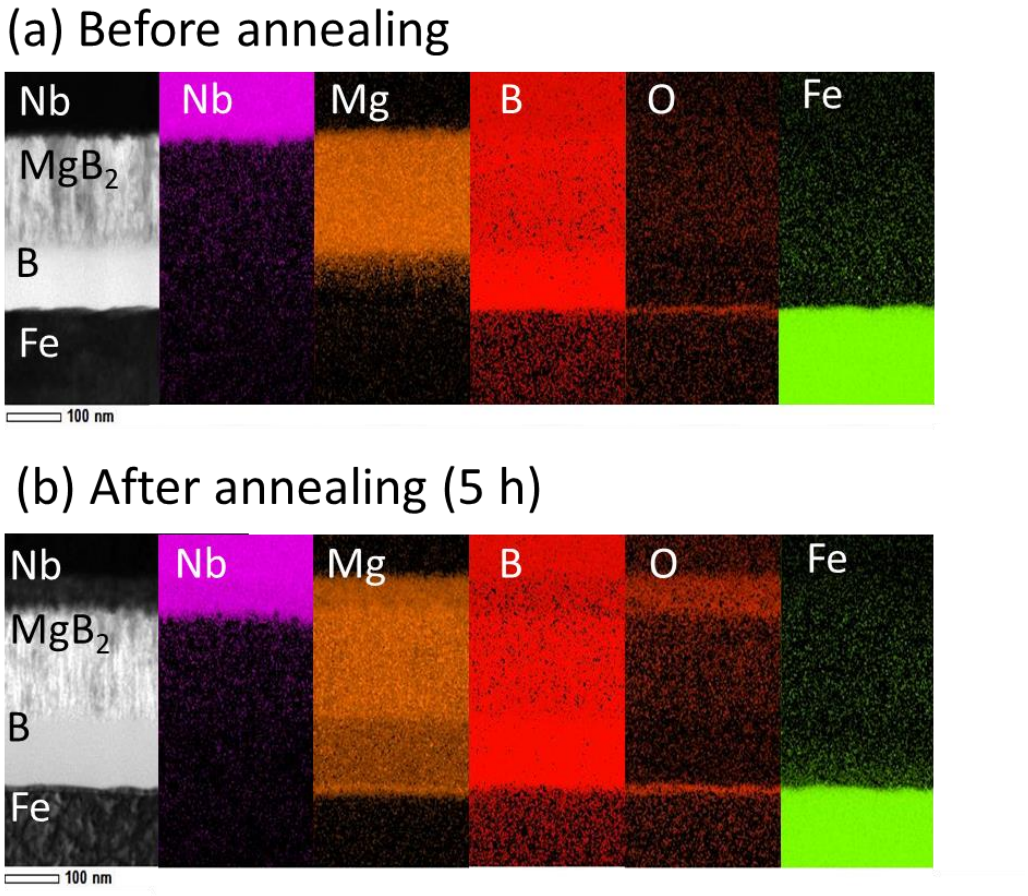
(a) Before annealing
Nb
MgB2
B
Fe
Nb
Mg
B
O
Fe
100 nm
(b) After annealing (5 h)
Nb
MgB2
B
Fe
Nb
Mg
B
O
Fe
100 nm

Fig. 4

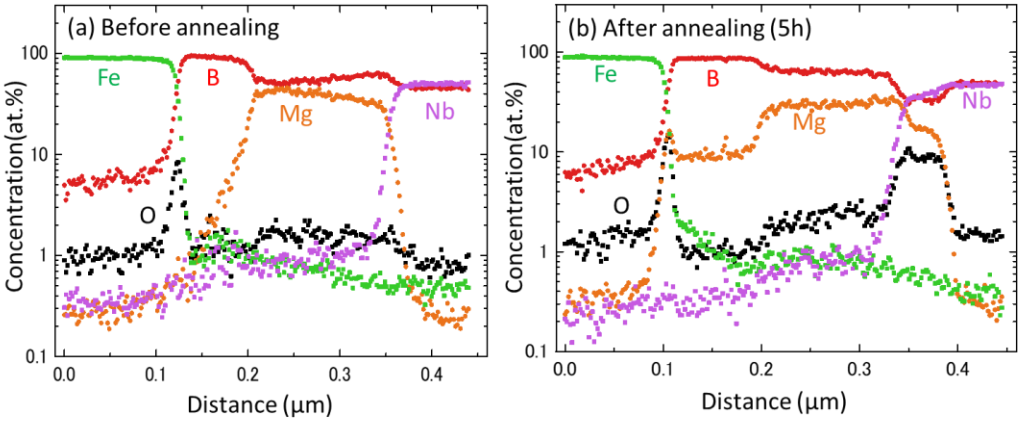
(a) Before annealing
(b) After annealing (5h)
Fe
B
Mg
Nb
O
Concentration(at.%)
Distance (μm)
100
10
1
0.1
0.0
0.1
0.2
0.3
0.4

Fig. 5